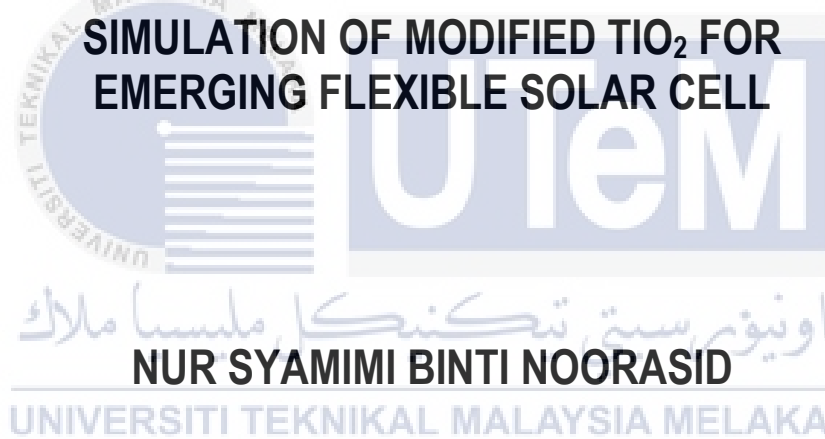




**SYNTHETIZATION AND NUMERICAL  
SIMULATION OF MODIFIED  $\text{TiO}_2$  FOR  
EMERGING FLEXIBLE SOLAR CELL**

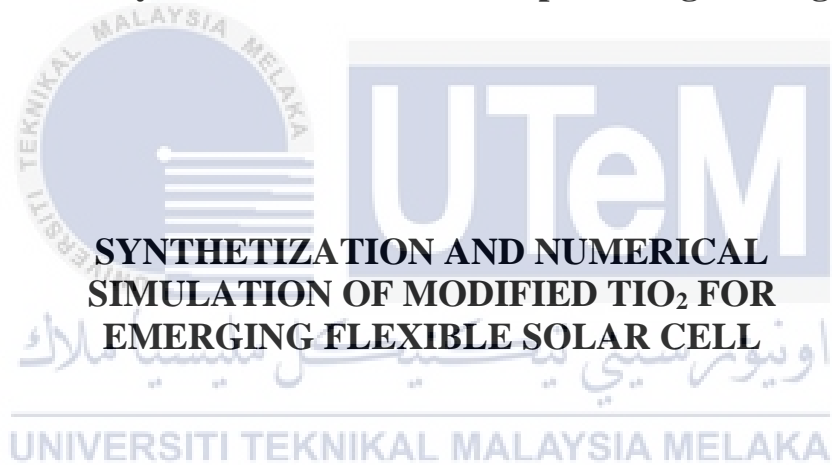


**MASTER OF SCIENCE IN ELECTRONIC  
ENGINEERING**

**2023**



**Faculty of Electronics and Computer Engineering**



**SYNTHETIZATION AND NUMERICAL  
SIMULATION OF MODIFIED  $\text{TiO}_2$  FOR  
EMERGING FLEXIBLE SOLAR CELL**

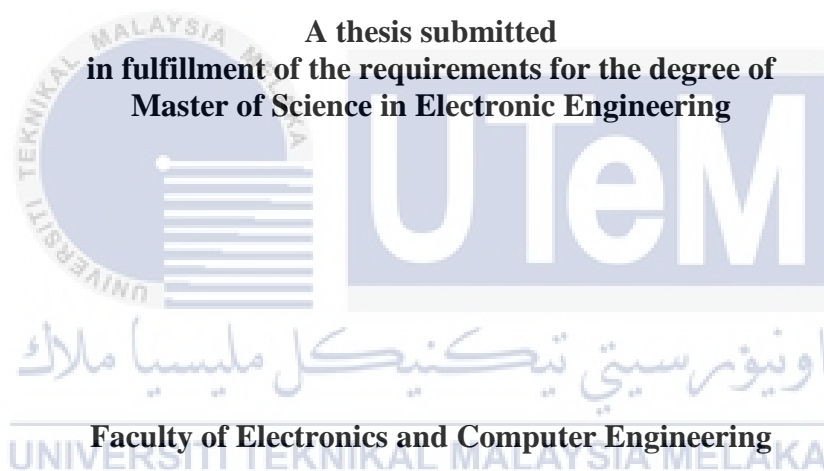
**Nur Syamimi Binti Nooraid**

**Master of Science in Electronic Engineering**

**2023**

**SYNTHETIZATION AND NUMERICAL SIMULATION OF MODIFIED  $\text{TiO}_2$   
FOR EMERGING FLEXIBLE SOLAR CELL**

**NUR SYAMIMI BINTI NOORASID**



**UNIVERSITI TEKNIKAL MALAYSIA MELAKA**

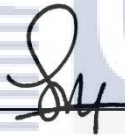
**2023**

## DECLARATION

I declare that this thesis entitled “Synthetization And Numerical Simulation Of Modified Tio<sub>2</sub> For Emerging Flexible Solar Cell” is the result of my own research except as cited in the references. The thesis has not been accepted for any degree and is not concurrently submitted in candidature of any other degree.

Signature

:



Name

:

Nur Syamimi Binti Noorasid

Date

:

12/04/2023



## APPROVAL

I hereby declare that I have read this thesis and in my opinion this thesis is sufficient in terms of scope and quality for the award of Master of Science in Electronic Engineering.

Signature

:

\_\_\_\_\_

Supervisor Name

:

Ts. Dr Faiz Bin Arith

Date

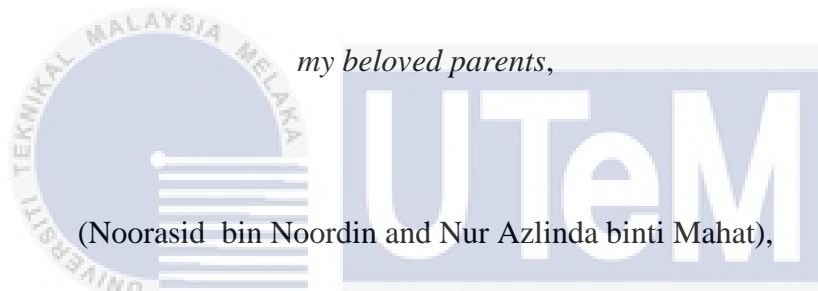
:

12/04/2023



## DEDICATION

This thesis is wholeheartedly dedicated to,



*my beloved parents,*

(Noorasid bin Noordin and Nur Azlinda binti Mahat),

who have been my source of inspiration and gave me strength when I thought of giving up,  
who continually provide their moral, spiritual, emotional, and financial support.

UNIVERSITI TEKNIKAL MALAYSIA MELAKA

*all of my siblings,*

(Muhammad Noor Hazwan bin Noorasid and Muhammad Noor Firdaus bin Noorasid)

who shared their words of advice and encouragement to finish this study.

*and all my relatives, mentor, lecturers, friends, and classmates,*

Thank you for supporting me during ups and downs in finishing my master study.

## ABSTRACT

Dye-Sensitized solar cells (DSSCs) have attracted massive attention due to simple and low-cost fabrication process. In addition, it also suitable to be used for indoor application. Compared to commercially available silicon-based solar cells, which require complicated equipment, higher cost and heavy, flexible DSSCs are lighter in weight, thinner, and lower fabrication cost. In conventional DSSCs structure, anatase ( $\text{TiO}_2$ ) has been used as a photoanode layer. However, the  $\text{TiO}_2$  paste required a high-temperature treatment ( $> 450^\circ\text{C}$ ) in order to obtain crystalline structure. The high-temperature process cannot be applicable to flexible DSSCs due to the flexible polymer substrates such as polyethylene terephthalate (PET) that are vulnerable to temperature, specifically below  $150^\circ\text{C}$ . This study has conducted two analyses based on experiment and simulation. Titanium dioxide ( $\text{TiO}_2$ ) layer was synthesized and deposited with varying concentrations of titanium tetrapropoxide (TTIP) within the range of 0.3–0.7 M using the sol gel and spin coat method during deposition onto flexible substrates (ITO/PET). The impact of TTIP concentration on the electrical, structural, and optical properties has been studied. Ultraviolet visible (UV-Vis) spectrum demonstrates that the visible transmittance of the  $\text{TiO}_2$  layer lies between 10% to 23% and direct band gap energy within the range from 3.08 eV to 3.49 eV. X-ray diffraction (XRD) spectrum revealed that the average size of  $\text{TiO}_2$  crystallites ranged from 4.35 to 5.23 nm. According to the IV curve, the current density obtained within the range of 0.0011  $\mu\text{A}$  to 0.0064 mA. Scanning electron microscopy (SEM) images for the concentration of 0.5 M achieved the most porosity structure than others. Thus, the layer of  $\text{TiO}_2$  with a concentration of 0.5 M TTIP demonstrates the ideal concentration of TTIP due to it high achievement of electrical, structural and optical properties. Next, the simulation carried out in this study used solar capacitance simulator (SCAPs) software and this simulation is based on the best band gap (3.2 eV) obtained from the experiment. Simulation part consists of 3 stages where all these stages use  $\text{TiO}_2$  as the main semiconductor material. The first stage is a simulation based on the DSSC structure. The simulation achieved efficiency of up to 8.14% by applying a 50 nm ultra-thin layer of  $\text{TiO}_2$  with a doping concentration of  $1 \times 10^{18} \text{ cm}^{-3}$  and the results show that the four factors (thickness, temperature, doping concentration and defect density) analyzed are highly influential in improving the efficiency of DSSC. The next stage is a simulation based on the SSDSSC structure. This simulation examined the performance of SSDSSC with a variety of ETLs, including  $\text{TiO}_2$ ,  $\text{ZnO}$ , and  $\text{SnO}_2$ . The simulation result indicates that the best ETL is  $\text{TiO}_2$ , with maximum efficiency of 5.6%. The last stage is a simulation based on the structure of the PSC. In this simulation, it is found that each layer affects the performance of the PSC and proves that the optimization of each layer effectively improves the performance of the PSC. Remarkable results of the optimized structure have achieved impressive PSC efficiency 28.30% by the parametric analysis. This study will lead the path and can be a guidance to increase and enhancing the performance of generation photovoltaic cells.

# **SINTESIS DAN SIMULASI BERANGKA $\text{TiO}_2$ TERUBAH SUAI UNTUK SEL SURIA FLEKSIBEL MEMUNCUL**

## **ABSTRAK**

Sel suria Peka Pewarna (DSSC) telah menarik perhatian besar-besaran kerana proses fabrikasi yang mudah dan kos rendah. Selain itu, ia juga sesuai digunakan untuk aplikasi dalaman. Berbanding dengan sel suria berasaskan silikon yang tersedia secara komersil, yang memerlukan peralatan yang rumit, kos yang lebih tinggi dan berat, DSSC yang boleh lentur adalah lebih ringan, nipis dan kos fabrikasi yang lebih rendah. Dalam struktur DSSC konvensional, anatase  $\text{TiO}_2$  telah digunakan sebagai lapisan fotoanod, di mana ia boleh memberikan struktur mesoporous yang sangat baik untuk penyerapan pewarna. Walau bagaimanapun, pes  $\text{TiO}_2$  memerlukan rawatan suhu tinggi ( $> 450\text{ }^\circ\text{C}$ ) untuk mendapatkan struktur kristal. Proses suhu tinggi tidak boleh digunakan untuk DSSC boleh lentur kerana substrat polimer boleh lentur seperti polietilena tereftalat (PET) yang terdedah kepada suhu, khususnya di bawah  $150\text{ }^\circ\text{C}$ . Kajian ini telah menjalankan dua analisis berdasarkan simulasi dan eksperimen. Lapisan titanium dioksida ( $\text{TiO}_2$ ) telah disintesis dan didepositkan dengan kepekatan titanium tetrapropoksida (TTIP) yang berbeza-beza dalam julat 0.3-0.7 M menggunakan kaedah sol gel dan spin coat semasa pempadaman ke substrat boleh lentur (ITO/PET). Kesan kepekatan TTIP terhadap sifat elektrik, struktur dan optik telah dikaji. Spektrum ultraviolet visible (UV-Visible) menunjukkan bahawa penghantaran kelihatan lapisan  $\text{TiO}_2$  terletak antara 10% sehingga 23% dan tenaga jurang jalur terus dalam julat dari 3.08 eV kepada 3.49 eV. Spektrum pembelauan sinar-x (XRD) mendedahkan bahawa anggaran saiz purata kristal  $\text{TiO}_2$  adalah antara 4.35 hingga 5.23 nm. Mengikut keluk IV, ketumpatan arus yang diperolehi dalam julat 0.0011  $\mu\text{A}$  to 0.0064 mA. Imej SEM untuk kepekatan 0.5 M mencapai struktur keliangan yang paling banyak daripada yang lain. Oleh itu, lapisan  $\text{TiO}_2$  dengan kepekatan 0.5 M TTIP menunjukkan penghantaran dan ketumpatan arus terbaik. Seterusnya, simulasi yang dijalankan dalam kajian ini menggunakan perisian solar capacitance simulator (SCAPs) dan simulasi ini adalah berdasarkan jurang jalur terbaik (3.2 eV) yang diperolehi daripada eksperimen. Simulasi ini terdiri daripada 3 peringkat di mana kesemua peringkat ini menggunakan  $\text{TiO}_2$  sebagai bahan semikonduktor utama. Peringkat pertama adalah simulasi berdasarkan struktur DSSC. Simulasi mencapai kecekapan sehingga 8.14% dengan menggunakan lapisan ultra-nipis 50 nm  $\text{TiO}_2$  dengan kepekatan doping  $1 \times 10^{18}\text{ cm}^{-3}$  dan keputusan menunjukkan bahawa empat faktor (ketebalan, suhu, kepekatan doping dan ketumpatan kecacatan) yang dianalisis sangat berpengaruh dalam meningkatkan kecekapan DSSC. Peringkat seterusnya ialah simulasi berdasarkan struktur SSDSSC. Dalam simulasi ini, prestasi SSDSSC dengan pelbagai ETL seperti  $\text{TiO}_2$ ,  $\text{ZnO}$ , dan  $\text{SnO}_2$  telah dikaji. Simulasi ini membuktikan  $\text{TiO}_2$  sebagai ETL memperoleh kecekapan terbaik sehingga 5.6%. Peringkat terakhir ialah simulasi berdasarkan struktur PSC. Dalam simulasi ini, didapati setiap lapisan mempengaruhi prestasi PSC dan membuktikan pengoptimuman setiap lapisan berkesan meningkatkan prestasi PSC. Keputusan luar biasa bagi struktur yang dioptimumkan telah mencapai kecekapan PSC yang mengagumkan sebanyak 28.30% dengan analisis parametrik. Kajian ini akan menerajui laluan dan boleh menjadi panduan untuk meningkatkan dan meningkatkan prestasi penjana sel fotovoltai.



## ACKNOWLEDGEMENT

In the Name of Allah, the Most Gracious, the Most Merciful

First of all, I would like to express my most profound appreciation to Dr. Faiz bin Arith, my principal supervisor, for his continuous support of my research, for his motivation, inspiration and patience throughout my MSc study. His guidance was precious to me during the research and writing of this thesis. He was always available for discussion, supervision, and support. I could not have imagined having a worthy advisor and mentor during my MSc studies.

Besides him, I would like to express my appreciation to Dr. Puvaneswaran Chelvanathan for sharing his expertise and guidance. He has been highly cooperative during my entire study. His continuous encouragement of my studies and critical and constructive comments sharpened my knowledge and research capabilities.

I would like to express my gratitude to UTeM for offering me the opportunity to study here. I would like to express my gratitude to all technical research staff at the Faculty of Electronic and Computer Engineering (FKEKK), the Faculty of Manufacturing Engineering (FKP), the Faculty of Electrical Engineering (FKE), and the Faculty of Mechanical and Manufacturing Engineering Technology (FTKMP) (all of which are operated by UTeM), especially those who assisted me with the characterization of my research.

I want to express my sincere thanks to all of my lab mates, colleagues, and friends for stimulating discussion and for all the fun we've had over the previous few years, which has made research interesting and time enjoyable and unforgettable at UTeM. Finally, I would like to express my gratitude to my beloved family for their spiritual support throughout my MSc and my life in general. I will never have enough words to describe my appreciation for my parents. This MSc is dedicated to my parents.

## TABLE OF CONTENTS

	PAGE
<b>DECLARATION</b>	
<b>DEDICATION</b>	
<b>ABSTRACT</b>	<b>i</b>
<b>ABSTRAK</b>	<b>ii</b>
<b>ACKNOWLEDGEMENTS</b>	<b>iii</b>
<b>TABLE OF CONTENTS</b>	<b>iv</b>
<b>LIST OF TABLES</b>	<b>vi</b>
<b>LIST OF FIGURES</b>	<b>vii</b>
<b>LIST OF APPENDICES</b>	<b>xii</b>
<b>LIST OF ABBREVIATIONS</b>	<b>xiii</b>
<b>LIST OF PUBLICATIONS</b>	<b>xvii</b>
<b>CHAPTER</b>	
<b>1. INTRODUCTION</b>	<b>1</b>
1.1 Research Background	1
1.2 Research Problem	2
1.3 Research Objectives	5
1.4 Scope of Work	5
1.5 Significance	6
1.6 Thesis Outline	6
<b>2. LITERATURE REVIEW</b>	<b>8</b>
2.1 Introduction	8
2.2 Solar Cell Terminology	11
2.2.1 Short Circuit Current( $I_{sc}$ )	11
2.2.2 Open-Circuit Voltage ( $V_{oc}$ )	11
2.2.3 Series Resistance ( $R_s$ )	12
2.2.4 Shunt Resistance ( $R_{SH}$ )	12
2.2.5 Fill Factor (FF)	13
2.2.6 Efficiency ( $\eta$ )	13
2.3 Flexible Dye-Sensitized Solar Cell	16
2.4 Type of Photoanode on Flexible-based	17
2.4.1 Zinc Oxide (ZnO)	17
2.4.2 Titanium Dioxide ( $TiO_2$ )	20
2.4.3 Graphene	29
2.5 Type of Photoanode in Glass-Based	34
2.5.1 Zinc Oxide (ZnO)	34
2.5.2 Titanium Dioxide ( $TiO_2$ )	36
2.5.3 Graphene	39
2.6 Fabrication Technique of FDSSC	40
2.6.1 Doctor Blade Deposition	41
2.6.2 Electrophoretic Deposition	42
2.6.3 Pulsed Laser Deposition (PLD)	44
2.6.4 Peel and Stick Process	46
2.6.5 Acetic Acid Gelation-Mechanical Press-Ammonia Activation (AG-MP-NA)	48
2.7 Recent Technology in FDSSC	49
2.8 Perovskite Solar Cell	54

2.9	Numerical Analysis Solar Cell	57
<b>3.</b>	<b>METHODOLOGY</b>	<b>61</b>
3.1	Introduction	61
3.2	Experimental of TiO <sub>2</sub> Layer	63
3.2.1	Synthesis of TiO <sub>2</sub>	63
3.2.2	Solution of Spin Coat	65
3.2.3	Deposition of TiO <sub>2</sub>	65
3.2.4	Characterization	66
3.3	Simulation of Dye-Sensitized and Perovskite Solar Cell	69
3.3.1	SCAPs 1D Software	69
3.3.2	Flowchart of SCAPs Software	71
3.3.3	Simulation of Ultrathin TiO <sub>2</sub> Photoanode of DSSCs	72
3.3.4	Simulation of SSDSSC Utilizing CuI as Hole Transport Layer	74
3.3.5	Simulation of Perovskite Solar Cell (PSC)	78
<b>4.</b>	<b>RESULT AND DISCUSSION FOR EXPERIMENTAL</b>	<b>85</b>
4.1	Experimental of TiO <sub>2</sub> on Flexible Substrate	85
4.1.1	Optical Analysis (UV-vis Spectrometer)	85
4.1.2	Electrical Analysis	89
4.1.3	Structure Analysis (XRD)	91
4.1.4	Structure Analysis (SEM)	97
4.2	Simulation Three Types of Third Generation of Solar Cell	99
4.2.1	Simulation of Ultrathin TiO <sub>2</sub> Photoanode of DSSCs	99
4.2.2	Simulation of SSDSSC Utilizing CuI as Hole Transport Layer	106
4.2.3	Simulation of Perovskite Solar Cell (PSC)	117
<b>5.</b>	<b>CONCLUSION AND RECOMMENDATIONS FOR FUTURE RESEARCH</b>	<b>140</b>
5.1	Conclusion	140
5.2	Recommendation	142
	<b>REFERENCES</b>	<b>143</b>
	<b>APPENDICES</b>	<b>163</b>

## LIST OF TABLES

TABLE	TITLE	PAGE
2.1	A summary of film preparation method for flexible and glass dye-sensitized solar cell	32
2.2	A summary of numerical analysis of solar cell	60
3.1	Amount of TTIP for various molar concentration (Ganghoffer, 2018)	63
3.2	Parameters of the component in device modelling of DSSC	73
3.3	Parameters of the component in device modelling of SSDSSC (Jahantigh and Safikhani, 2019)	76
3.4	Parameter of various material of ETL	76
3.5	Parameters of the absorber layer in device modelling of SSDSSC	77
3.6	Work Function of Metal	81
3.7	Basic Parameters of $\text{CH}_3\text{NH}_3\text{SnI}_3$ of PSC	81
3.8	Basic Parameters of various HTL of $\text{CH}_3\text{NH}_3\text{SnI}_3$ PSC	82
3.9	Total defect density at the interface and inside absorber layer	83
4.1	Data of interplanar spacing and miller indices	92
4.2	The lattice constant of standard and calculation value for various concentration of TTIP	94
4.3	The value of crystallite size, dislocation density and lattice strain for various concentration of TTIP	95
4.4	Comparison lattice strain value with previous paper	96

## LIST OF FIGURES

FIGURE	TITLE	PAGE
2.1	Schematic of (a) layer and (b) basic operating principle of DSSC (Sharma et al., 2018)	8
2.2	Band diagram of different metal oxide material (Mohiuddin et al., 2018)	9
2.3	IV characteristic curve of a photovoltaic cell with (a) high FF, (b) low FF and (c) Pmax identification (Dittrich, 2018)	15
2.4	(a) SEM image of TiO <sub>2</sub> ; (b) SEM image of ZnO coated TiO <sub>2</sub> powder; (c) IV characteristic for both flexible DSSCs (Kim et al., 2005)	18
2.5	SEM images of a single layer structure film (a, b); a double layer composite film (c, d) (Chen et al., 2010a)	18
2.6	IV characteristic with (a) electrophoresis deposition (EPD); (b) solid state reaction (Chen et al., 2011c; Yin et al., 2012)	19
2.7	(a) IPCE spectra of red dye, black dye and relative photon flux of sunlight (A.M 1.5 G). (b) IPCE red and black dye containing 4-tert-butylpyridine (Lee et al., 2018)	21
2.8	FESEM image of 19 nm particle (a) as prepared EPD film; (b) after compression; (c) IV characteristic of flexible DSSCs (Xue et al., 2012)	22
2.9	(a) and (b) TEM images of small and big nanowire. (c) FESEM image of free standing flexible TiO <sub>2</sub> nanowire film showing small and big nanowire layered structure (Wang et al., 2012)	23
2.10	SEM image of the flexible TiO <sub>2</sub> film with stirring time (a) 24h; (b) 48h and amount of TTIP with molar percentage of (c) 6%; (d) 10% (Wang et al., 2011)	24
2.11	SEM image of TiO <sub>2</sub> photoelectrode with (a) non pressed; (b) pressed under 100 Mpa (Yamaguchi et al., 2010)	25

2.12	SEM images of TiO <sub>2</sub> film (a) as deposited; (b) pressed under 100 MPa. MPa.; (c) IV characteristic of different nanocomposite gel (Lee et al., 2013b)	26
2.13	Absorbance data (a) hibiscus leachate with ethanol (b) hibiscus leachate with water of flexible DSSCs (Cao et al., 2021)	27
2.14	IV-characteristic of flexible DSSC with different ratio of TiO <sub>2</sub> (Poh et al., 2021)	28
2.15	(a) SEM image of a 3D graphene foam.; (b) Cross sectional FESEM of 3DGT 0.85 film. (c) IV characteristic based on the 3DGT 0.5, 3DGT - (Zhi et al., 2015)	30
2.16	IV- characteristic of bare photoanode, bare photoanode + G LSL, bare photoanode + T LSL and bare photoanode + TG LSL (Mustafa and Sulaiman, 2020)	31
2.17	SEM images of the films deposited by (a) laser ablation and (b) doctor blade method (Sima et al., 2015)	35
2.18	(a) SEM image of 10mM concentration of synthesized ZnO and (b) IV curve of various concentration of synthesized ZnO (Meng et al., 2014)	36
2.19	IV curve with various standby time of (a) 1 hours and (b) 2 hours loading time (Aksoy et al., 2019)	36
2.20	Cross section SEM images of TiO <sub>2</sub> layer with (a) doctor blade and (b) inkjet printing method (Kunugi et al., 2013)	37
2.21	IV curve of various TiO <sub>2</sub> photoanode (Shao et al., 2014)	38
2.22	Analysis result for photoanode (a) dye loading and (b) IV curve with different porosities of photoanode (Zatirostami, 2021)	39
2.23	IV curve of f TiO <sub>2</sub> NPs and sensitized TiO <sub>2</sub> NPs as photoanodes in DSSCs (Jahantigh et al., 2020)	40
2.24	Schematic illustration of doctor blade (Hamzah et al., 2018)	41
2.25	Schematic illustration of EPD technique (Lee et al., 2012)	43
2.26	Schematic presentation of PLD technique (Grant-Jacob et al., 2018)	45
2.27	Debond growth behaviour of the Ni/SiO <sub>2</sub> interface (Lee et al., 2013a)	47
2.28	Schematic of the "AG MP NA" technique (Chen et al., 2010a)	48
2.29	Crystallite size of TiO <sub>2</sub> thin film with different TTIP molarity (Shuhadah et al., 2018)	50

2.30	FESEM images of different TTIP molarity (a) 0.2 M; (b) 0.4 M; (c) 0.8 M; (d) 1.0 M (Hafizah et al., 2012)	51
2.31	Upper SEM images from 1 mol to 3 mol of TTIP (Fagnern et al., 2012)	52
2.32	TEM images of TiO <sub>2</sub> films with different concentrations of TTIP (a) 0.041 mol L <sup>-1</sup> (3D hierarchical structure), (b) 0.082 mol L <sup>-1</sup> (nanosheet), (c) 0.10 mol L <sup>-1</sup> (nanoflakes and nanowire), (d) 0.12 mol L <sup>-1</sup> (long nanowire and nanoparticles) (Sun et al., 2021)	54
2.33	Typical crystal structure (unit cell) of perovskite material (Adjogri and Meyer, 2020)	55
2.34	Geometry system of TiO <sub>2</sub> and CH <sub>3</sub> NH <sub>3</sub> SnI <sub>3</sub> (Long et al., 2017)	56
2.35	Schematic of the basic working principle of perovskite solar cells (Ali, 2019)	57
3.1	The flowchart of the whole research	62
3.2	The flowchart of TiO <sub>2</sub> synthesis process	64
3.3	The schematic process of synthesis TiO <sub>2</sub>	64
3.4	The schematic deposition process of TiO <sub>2</sub> via spin coat technique	65
3.5	Panels description of SCAPs (a) action panel, (b) definition panel and (c) layer properties	70
3.6	Flowchart of SCAPs simulation	72
3.7	The simulated device structure of SSDSSC (Jahantigh and Safikhani, 2019)	75
3.8	Band alignment (relative to vacuum level) of simulated device structure of SSDSSC (Jahantigh and Safikhani, 2019)	75
3.9	Lead-free solar cell (a)conventional structure (b) optimized structure	80
3.10	Energy level diagram of CH <sub>3</sub> NH <sub>3</sub> SnI <sub>3</sub> PSC	80
4.1	Absorbance peak of various concentration of TTIP	86
4.2	Transmittance peak for various concentration of TTIP	87
4.3	Direct bandgap for various concentration of TTIP	88
4.4	IV curve of various concentration of TTIP	89
4.5	The curve of conductance and resistance with various concentration of TTIP	90

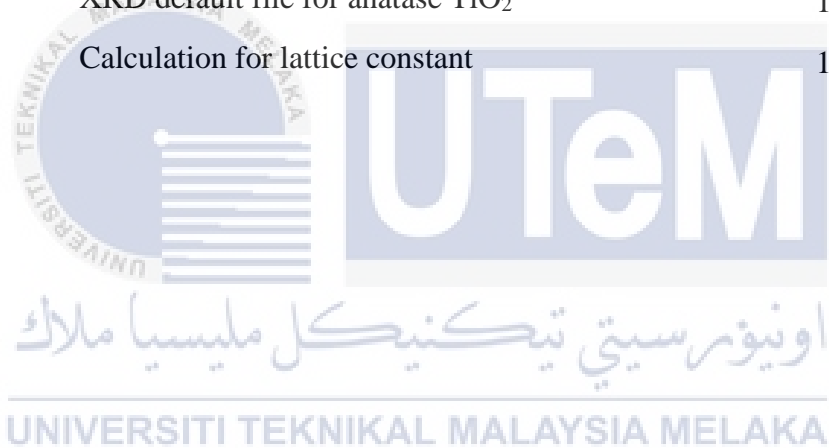
4.6	XRD pattern for variation concentration of TTIP	91
4.7	The pattern of crystallite size, lattice strain and dislocation density for various concentration of TTIP	96
4.8	SEM images with $\times 20$ magnification for (a) 0.3 M, (b) 0.5 M and (c) 0.7 M	98
4.9	SEM images with $\times 500$ magnification for (a) 0.3 M, (b) 0.5 M and (c) 0.7 M	99
4.10	The effect of $\text{TiO}_2$ layer thickness on (a) open-circuit voltage ( $V_{oc}$ ), (b) short-circuit current (JSC), (c) fill factor (FF) and (d) efficiency (PCE) of the DSSC	100
4.11	The efficiency (PCE) of DSSC at different operating temperature	102
4.12	The efficiency (PCE) of DSSC with different doping concentration	103
4.13	The efficiency (PCE) vs (a) neutral, (b) donor and (c) acceptor defect density at $\text{TiO}_2/\text{N719}$ interlayer of the DSSC	104
4.14	The optimum thickness CuI thickness of device with and without the presence of Ni as a back contact on the efficiency of SSDSSC	107
4.15	(a) The variation of CuI doping acceptor density with and without the presence of Ni as a back contact on the efficiency of SSDSSC; The recombination rate of SSDSSC (b) without and (c) with back contact based on the variation of doping acceptor density	109
4.16	The variation of working temperature with and without the presence of Ni as a back contact on the efficiency of SSDSSC	110
4.17	The variation of back contact material on the efficiency of SSDSSC	111
4.18	(a) The variation of defect interface 1 and 2 with and without the presence of Ni as a back contact on the efficiency of SSDSSC. The recombination rate of SSDSSC on the variation (b) at interface defect at $\text{CuI}/\text{N719}$ ; (c) at $\text{N719}/\text{TiO}_2$	113
4.19	(a) IV curve; (b) quantum efficiency for the variation of absorber layer for SSDSSC with back contact	115
4.20	(a) IV curve; (b) recombination rate of the performance of SSDSSC with back contact under dark and light illumination	116
4.21	Dark vs Illumination IV Characteristic	118
4.22	IV characteristics of PSC with various thickness of $\text{TiO}_2$	120



4.23	Influence of operating temperature on (a) Various efficiency of PSC with temperature for various thickness of TiO <sub>2</sub> ; (b) IV curve between operating temperature of 300 K and 400 K	122
4.24	Various efficiency of PSC with neutral defect density of TiO <sub>2</sub> for various thickness of TiO <sub>2</sub>	123
4.25	Various efficiency of PSC with various thickness of absorbance for lead-free (CH <sub>3</sub> NH <sub>3</sub> SnI <sub>3</sub> ) and lead-based (CH <sub>3</sub> NH <sub>3</sub> PbI <sub>3</sub> ) perovskite	125
4.26	Performance parameter of PSC with various thickness of absorber layer	126
4.27	(a) Performance parameter and (b) Recombination rate with various acceptor concentration of absorber layer	128
4.28	Performance of PCE based on hole capture cross section	130
4.29	Performance of PSC based on (a) PCE and (b) recombination rate with various defect density of absorber layer	132
4.30	Performance of PSC based on PCE with various defect density at interface (a) Abs/ETL and (b) HTL/Abs	133
4.31	Performance PV parameter of HTL candidates with various layer thickness	135
4.32	Band alignment of HTL candidates	135
4.33	Band alignment of various metal work function	137
4.34	PV parameter of PSC with various metal work function	138

## LIST OF APPENDICES

APPENDIX	TITLE	PAGE
A	Experimental for TiO <sub>2</sub> layer	163
B	Absorbance edge spectrum graph	172
C1	XRD default file for anatase TiO <sub>2</sub>	174
C2	Calculation for lattice constant	179



## LIST OF SYMBOLS

AZO	-	Aluminium Zinc Oxide
AG-MP-NA	-	Acetic Acid Gelation-Mechanical Press-Ammonia Activation
Ag-NW	-	Silver Nanowire
Au	-	Gold
C <sub>2</sub> H <sub>3</sub> OH	-	Ethanol
C <sub>2</sub> H <sub>6</sub> O <sub>2</sub>	-	Ethylene Glycol
CB	-	Conduction Band
CdTe	-	Cadmium telluride
CH <sub>3</sub> COOH	-	Acetic Acid
CH <sub>3</sub> NH <sub>3</sub> PbI <sub>3</sub>	-	Methylammonium Lead Halide
CH <sub>3</sub> NH <sub>3</sub> SnI <sub>3</sub>	-	Methylammonium Tin Iodide
CIGS	-	Copper Indium Gallium Selenide Solar Sells
CIP	-	Cold Isostatic Compression
Cr	-	Chromium
CSCNT	-	Cup-Stacked Carbon Nanotubes
Cu	-	Copper
CuI	-	Copper (I) Iodide
CuSCN	-	Copper Thiocynate
CVD	-	Chemical Vapor Deposition
D	-	Crystallite Size
DFT	-	Density Functional Theory
DGT	-	Double-Graphene-Tubes
DSSC	-	Dye-Sensitized Solar Cell
Ec	-	Conduction Band
Eg	-	Bandgap

Ev	-	Valence Band
EPD	-	Electrophoretic Deposition
ETL	-	Electron Transport Layer
eV	-	Electron Volt
FDSSC	-	Flexible Dye-Sensitized Solar Cell
FESEM	-	Field Emission Scanning Electron Microscope
FF	-	Fill Factor
FPSC	-	Flexible Perovskite Solar Cell
FTO	-	Fluorine doped Tin Oxide
GQD	-	Graphene Quantum Dot
Gr	-	Graphene
HOMO	-	Highest Occupied Molecular Orbit
HTL	-	Hole Transport Layer
HTM	-	Hole Transport Material
Im	-	Maximum Current
IPCE	-	Incident Photon-to-Electron Conversion Efficiency
Isc	-	Short Circuit Current
ITO	-	Indium Tin Oxide
IV	-	Current - Voltage
Jo	-	Saturation Current
Jsc	-	Current Density
K	-	Scherrer Constant
KI	-	Potassium Iodide
LSL	-	Light Scattering Layer
LUMO	-	Lowest Unoccupied Molecular Orbit
MAPbI <sub>3</sub>	-	Methylammonium Lead Iodide
MD	-	Molecular Dynamic
Mo	-	Molybdenum
MoO <sub>3</sub>	-	Molybdenum Trioxide
MPa	-	Megapascal
MWCNT	-	Multi-Wire Carbon Nanotube
N <sub>3</sub>	-	Nitride
N719	-	Ruthenizer

$N_A$	-	Acceptor Density
$N_C$	-	Density of Charge at Conduction Band
$N_{CB}$	-	Effective State Density
$N_D$	-	Donor Density
$N_t$	-	Defect Density
$NH_3$	-	Ammonia
Ni	-	Nickel
NP	-	Nanoparticle
NR	-	Nanorod
NRP	-	Nanorods Particle
$N_V$	-	Density of Charge at Valence Band
NW	-	Nanowire
PCBM	-	Phenyl-C61-Butyric acid Methyl ester
PCE	-	Power Conversion Efficiency
PEDOT:PSS	-	poly(3,4-ethylenedioxythiophene) polystyrene sulphonate
PEN	-	Polyethylene naphthalate
PES	-	Polyethersulfone
PET	-	Polyethylene terephthalate
PLD	-	Pulse Laser Deposition
PSC	-	Perovskite Solar Cell
Pt	-	Platinum
PTAA	-	poly[bis(4 phenyl)(2,4,6-trimethylphenyl)amine]
PV	-	Photovoltaics
PVD	-	Physical Vapour Deposition
$R_{SH}$	-	Shunt Resistance
SCAPs	-	Solar cell Capacitance Simulator Software
SEM	-	Scanning Electron Microscope
SLGQD	-	Single-Layer Graphene Quantum Dots
$SnIn_2O_3$	-	Indium Tin Oxide/Polyethylene terephthalate
$SnO_2$	-	Tin Oxide
SRH	-	Shockley–Read–Hall
SSDSSC	-	Solid State Dye-Sensitized Solar Cell
Spiro Ometad	-	2,2',7,7-tetrakis(N,N-pdimethoxyphenylamino)-9,9'-

	-	pirobifluorene;
TCO	-	Transparent Conducting Oxide
TEM	-	Transmission Electron Microscopy
TG	-	Titanium Dioxide-Graphene Quantum Dot
TiO <sub>2</sub>	-	Titanium Dioxide
TTIP	-	Titanium Isopropoxide
UV	-	Ultraviolet
UV-O <sub>3</sub>	-	Ultraviolet–ozone
UV-Vis	-	Ultraviolet–Visible Spectroscopy
V <sub>2</sub> O <sub>5</sub>	-	Vanadium Pentoxide
V <sub>B</sub>	-	Valence Band
V <sub>m</sub>	-	Voltage Maximum
V <sub>oc</sub>	-	Open Circuit Voltage
WTP	-	Water-Assisted Transfer Printing
XPS	-	X-ray photoelectron spectroscopy
XRD	-	X-ray Diffraction
YBa <sub>2</sub> Cu <sub>3</sub> O <sub>7</sub>	-	Yttrium barium copper oxide
Zn(NO <sub>3</sub> ) <sub>2</sub>	-	Zinc Nitrate
ZnO	-	Zinc Oxide
$\alpha$	-	Alpha (absorption coefficient)
$\epsilon_r$	-	Relative Permittivity
$\chi$	-	Electron Affinity
$\mu_m$	-	Micrometre
$\mu_n$	-	Electron Mobility
$\mu_p$	-	Hole Mobility
$a, c$	-	Lattice Constant
$hkl$	-	Miller Indices
$d$	-	Interplanar Spacing
$\mathcal{E}$	-	Lattice Strain
$\theta$	-	Angle
$\lambda$	-	Radiation Wavelength

## LIST OF PUBLICATIONS

1. **N. S. Nooraid**, F. Arith, A.N. Mustafa, P. Chelvanathan, MI Hossain and N. Amin, Improved performance of lead-free Perovskite solar cell incorporated with TiO<sub>2</sub> ETL and CuI HTL using SCAPS. *Applied Physics A: Materials Science and Processing* 129(2), 2023, pp. 1–16.(WoS Q2 IF:2.983 and Scopus Indexed)
2. **N. S. Nooraid**, F. Arith, A. Y. Firhat, A. N. Mustafa, and A. S. M.Shah, SCAPS Numerical Analysis of Solid-State Dye-Sensitized Solar Cell Utilizing Copper (I) Iodide as Hole Transport Layer, *Engineering Journal*, vol. 26, no. 2, pp. 1-10, Feb. 2022 (WoS ESCI and Scopus Indexed).
3. **N.S. Nooraid**, F. Arith, A.N. Mustafa, M.A. Azam, S. Mahalingam, P. Chelvanathan, N. Amin, Current Advancement of Flexible Dye Sensitized Solar Cell: A Review, *Optik*, Volume 254,2022,168089,ISSN 0030-4026. (WoS Q2 IF:2.443 and Scopus Indexed).
4. **N. S. Nooraid**, F. Arith, A. N. M. Mustafa, S. H. M. Suhaimy, A. S. Mohd Shah and M. A. Mohd Abid, "Numerical Analysis of Ultrathin TiO<sub>2</sub> Photoanode Layer of Dye Sensitized Solar Cell by Using SCAPS-1D," *2021 IEEE Regional Symposium on Micro and Nanoelectronics (RSM)*, 2021, pp. 96-99.

UNIVERSITI TEKNIKAL MALAYSIA MELAKA

# CHAPTER 1

## INTRODUCTION

### 1.1 Research Background

As the world is becoming more advanced in economy and technology, more energy is being consumed to keep up with the development and demand on energy boomed over past decades. Presently, the energy demands are still highly dependent on fossil fuels, natural gases and coal with percentages of 31.2%, 24.7% and 27.2% respectively (bp, 2022). However, the world will shortly come to an end of fossil fuels due to its non-renewable. Meanwhile, the wasteful use of fossil fuels actually causes irreversible environmental damage, geopolitical tensions, and tragically climate changes (Kabeyi and Olanrewaju, 2022). Our world definitely must move toward a more sustainable energy economy. Of all the available technologies to produce renewable energy, solar energy has become a hot topic in current research for replacing fossil fuels. One simple reason is that the earth receives  $1.2 \times 10^{17}$  W insolation or  $3 \times 10^{24}$  Joule energy per year from the sun and this means covering only 0.13% of the Earth's surface with solar cells with an efficiency of 10% would satisfy humanities' energy needs (Edward et al., 2019). Apart from the abundance of potentially exploitable solar energy, photovoltaic cells also have other competitive advantages such as little need for maintenance, off-grid operation and silence, which are ideal for usage in remote sites or mobile applications (Kabeyi and Olanrewaju, 2022). Currently, mankind has made use of three main ways of converting sunlight to a useable source of energy.